Int. J. Multiphase Flow, Vol. 3, pp. 273–283. Pergamon/Elsevier, 1977. Printed in Great Britain.

THE WAVY ASPECT OF A HORIZONTAL CO-CURRENT AIR–WATER FILM FLOW AND THE TRANSPORT PHENOMENA

V. PIMSNER and P. TOMA

Aerospace Department, Politechnical Institute, Bucharest and Alberta Research Council, Product Research and Development, Edmonton, Canada

(*Received* 5 *November* 1974)

Abstract—New experimental equations are developed for local void fraction, shear stress and net heat-transfer coefficient in a horizontal two-phase flowing system. Starting from statistically analysed wavy film motion, a simplified model is constructed enabling the correlation of the observed transport phenomena. The analytical description is based on the well known "law of the wall" equations, thus offering a unique description of the system.

1. INTRODUCTION

A great amount of research has dealt with heat transfer rates and pressure losses in two-phase gas–liquid systems. Unfortunately, the conclusions of some of these experimental and theoretical works have been contradictory or limited regarding the prediction of heat-transfer and pressure-loss coefficients.

In spite of the fact that the wavy aspect of the gas–liquid interface has been thoroughly investigated (Hanratty & Engen 1957; Ostrach & Koestel 1965; Gater & L'Ecuyer 1970; Telles & Dukler 1970) its interference with some specific transport phenomena is still considered an open problem. The transitions from two-dimensional waves to a squall surface and then to disturbance waves (also called roll waves in vertical systems) are related with sophisticated stability analyses that seems to remove these aspects from the engineering realm of practical computations.

The research reported herein is an attempt to analyse both the turbulent flow and wavy interface mechanism in a co-current air–water flow system with heat transfer.

2. RELATED MASS-, MOMENTUM- AND HEAT-TRANSFER STUDIES

It is generally agreed that wavy motion enhances the interfacial mass- and heat-transfer (Chang & Dukler 1964; Frisk & Davis 1972). The experimental study performed by Frisk & Davis (1972) shows an increase of the Nusselt number by more than 100% when the waves are noticeable as compared with a smooth film–gas flow. The suppression of the wave was possible by means of a surfactant introduced in the water, but in this case a new wave forming mechanism related to the surface tension value must be considered.

By assuming a combination of molecular and eddy transport of heat and momentum, the Dukler theory (1960) stands as a reference basis for many experimental studies in two-phase liquid film flows, Clegg & Tait (1962). The solution of the transport equations depends on the way the turbulent transport terms are expressed. Dukler (1960) used the Deissler (1955) and von Karman equations for the region of the film closest to the wall and for the farther regions respectively. Biasi *et al.* (1968) have used similar considerations in analysing a two-phase annular system with a homogeneous core in order to determine the velocity distribution and film thickness. The use of the above mentioned theories of Dukler and Biasi depends on the knowledge or computation (Lockhart & Martinelli 1949) of the total pressure drop in the system.

Levy (1966) had previously found an analytical solution of the two-phase annular flow with liquid entrainment by determining a function depending on the film thickness. The changing of interaction between the phases induced by wavy geometry was not considered in terms of the aforementioned theories and that is why the direct mechanism of phase interaction could not be evinced.

The wave propagation which induces a pulsation in the system was also analysed by Chang & Dukler (1964). It is quite difficult to distinguish either the contribution of pulsation from that of the boundary shear, or the contribution of the reversed flow due to the separation phenomena (at the crests of waves) to the improvement of the considered transport mechanism.

3. A SIMPLIFIED MODEL FOR THE TWO-PHASE FILM FLOW

A model was constructed which allowed the possibility of introducing in the classical turbulent boundary layer theories some characteristic aspects such as: the wavy interface, droplet generation and interface interaction.

The basic equations applied to a well established continuous flow region, written in dimensionless form (where index "o" is denoted the wall condition) are:

$$\frac{\tau_y}{\tau_0}=\left(\frac{\nu}{\nu_0}+\frac{\epsilon}{\nu_0}\right)\left[\frac{\rho}{\rho_0}\frac{dw^+}{dy^+}+w^+\frac{d(\rho/\rho_0)}{dy^+}\right], \qquad [1]$$

τ the fluid shear stress, ν kinematic viscosity, ρ density, ϵ eddy viscosity, y^+ stands for dimensionless distance ($y^+\equiv w^*y/\nu$) where w^* is friction velocity [$w^*\equiv\sqrt{(\tau/\rho)}$] and w^+ stands for dimensionless velocity ($w^+=w/w^*$). By denoting dimensionless temperature $T^+\equiv(T_0-T)C_{p0}\tau_0/q_0\sqrt{(\tau_0/\rho_0)}$, and heat-transfer parameter $\beta\equiv q_0\sqrt{(\tau_0/\rho_0)}/C_{p0}\tau_0T_0\rho_0$, the heat-transfer equation is written:

$$\frac{q}{q_0}=\left(\frac{\nu}{\nu_0}\frac{1}{Pr_0(Pr/Pr_0)}+\frac{\epsilon h}{\nu_0}\right)\times$$
$$\times\left[\left(\frac{\rho C_p}{\rho C_{p0}}\right)\frac{dT^+}{dy^+}+\left(T^+-\frac{1}{\beta}\right)\frac{d(\rho C_p/\rho_0C_{p0})}{dy^+}\right], \qquad [2]$$

where Pr is the Prandtl number.

The total shear equation [1] and the heat-transfer equation [2] are not restricted to a constant density fluid or to a linear or constant shear stress and heat-flux distribution (Deissler 1955). In the previously analysed one phase flow in hydraulically smooth ducts:

$$\frac{d(\rho/\rho_0)}{dy^+}=0;\quad \frac{Pr}{Pr_0}=1;\quad \frac{\tau_y}{\tau_0}=1;\quad \frac{\rho}{\rho_0}=1. \qquad [3a, b, c]$$

The relations [1] and [2] could be thus reduced to the well known form used by Deissler (1955) in the heat-transfer analysis:

$$1=\left(\frac{\mu}{\mu_0}+\frac{\rho}{\rho_0}\frac{\epsilon}{\epsilon_0}\right)\frac{dw^+}{dy^+}, \qquad [4]$$

$$1=\left(\frac{\lambda}{\lambda_0}\frac{1}{Pr_0}+\frac{\rho}{\rho_0}\frac{\epsilon}{\lambda_0}\right)\frac{dT^+}{dy^+}. \qquad [5]$$

In order to apply [1] and [2] to the dispersed flow region a void fraction model is to be adopted. Using the homogeneous hypothesis the parameters are written as:

$$\rho_{2F}\equiv\alpha\rho_G+(1-\alpha)\rho_L;\quad (\rho C_p)_{2F}\equiv\alpha(\rho C_p)_G+(1-\alpha)(\rho C_p)_L;$$
$$Pr_{2F}\equiv\alpha Pr_G+(1-\alpha)Pr_L;\quad \nu_{2F}\equiv\alpha\nu_G+(1-\alpha)\nu_L\quad \text{etc,}. \qquad [6a, b, c, d]$$

where α is the void fraction, subscript G is for the gas, L for the liquid and $2F$ for two-phase, droplet–gas core flow.

A developed model, as for example a "constant slip" one (Dukler *et al.* 1964) could be also used, but in this case the equations become too sophisticated. For the parameters characterizing a state far from the critical one (in the two phase one component system or in an air–water one) e.g. $\rho_L \gg \rho_G$, it could be also assumed that $(\rho C_p)_L \gg (\rho C_p)_G$ and $\nu_L \gg \nu_G$. For $Pr_L > Pr_G$ it is also necessary that $\beta > 0$ and boiling be avoided.

Equations [1] and [2] can be thus rewritten as:

$$\frac{\tau_y}{\tau_0} = \left[(1-\alpha)\frac{\nu_L}{\nu_0} + \frac{\epsilon}{\nu_0}\right]\left\{(1-\alpha)\frac{\rho_L}{\rho_G}\frac{dw^+}{dy^+} + w_y^+\left[\frac{d(\rho_L/\rho_G)}{dy^+}(1-\alpha) - \frac{\rho_L}{\rho_G}\frac{d\alpha}{dy^+}\right]\right\}, \quad [7]$$

$$\frac{q}{q_0} = \left[\frac{\nu_L}{\nu_0}\frac{(1-\alpha)}{Pr_0(Pr_L/Pr_0)} + \frac{\epsilon h}{\nu_0}\right]\left\{(1-\alpha)\frac{(\rho C_p)_L}{(\rho C_p)_0}\frac{dT^+}{dy^+} + \left(T^+ - \frac{1}{\beta}\right)\times\right. \quad [8]$$

$$\left.\times\left[\frac{d\,(\rho C_p)_L/(\rho C_p)_0}{dy^+}(1-\alpha) - \frac{(\rho C_p)_L}{(\rho C_p)_0}\frac{d\alpha}{dy^+}\right]\right\}.$$

Equations [7] and [8] for a two phase turbulent system are so far undetermined.

A new model and an experimental analysis were developed with the goal of solving these equations.

At this stage, instead of real waves, a sinusoidal interface was assumed as is schematically shown in figure 1.

The model and the real flow have in common both the same time average height of the film $\bar{h}$ defined as:

$$\bar{h} = \lim_{T\to\infty}\frac{1}{T}\int_0^T y\,dT, \quad [9]$$

and the variance of height designated by y_{eff}, defined as the root mean-squared value of the fluctuating quantity y' of height:

$$y_{eff} = (\bar{y'^2})^{1/2} = \left[\lim_{T\to\infty}\frac{1}{T}\int_0^T y'^2\,dT\right]^{1/2}. \quad [10]$$

The two distinct zones in the above defined model are:—the continuous liquid zone ($\alpha = 0$), $0 \leqslant y^+ \leqslant y^+_{min}$ – the dispersed zone ($0 < \alpha < 1$), $y^+ > y^+_{min}$.

In this way, it is assumed that void fraction α is continuously varied from the wavy region to the dispersed core flow.

For the sinusoidal form of the wave model, the maximum and minimum film heights are:

$$y_{max} = \bar{h} + y_{eff},$$

$$y_{min} = \bar{h} - y_{eff}. \quad [11a, b]$$

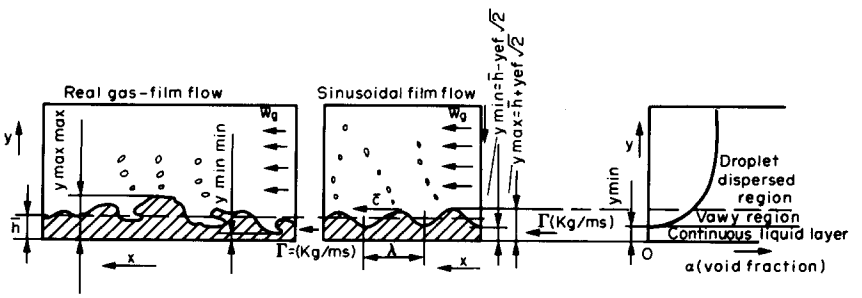

Figure 1. The model and the notation used.

The fraction of liquid in waves (Telles & Dukler 1970) used as a wavy form factor is defined:

$$X = \frac{y_{\text{eff}}\sqrt{(2)}}{\bar{h}}. \qquad [12]$$

This factor is thus easily determined provided that the value of y_{eff} and $\bar{h}$ are known from experimental statistical analysis.

By using both the data supplied by Lilleleht & Hanratty (1961) and some of Pimsner & Toma (1970) for an air–water film flowing in a horizontal channel, the function X can be formulated in terms of Re_L, Re_G and We (for the bulk film temperature),

$$X = 0.22\left[We \ln\frac{Re_G}{Re_L}\right]^{0.589} \qquad [13]$$

in the range of $0.1 < X < 0.8$; where the gas Reynolds number is $Re_G = \bar{w}_G D_h/\nu_G$, the liquid is $Re_L = 4\Gamma/\nu_L$, and the Weber number is $We = \bar{w}_G^2\rho_G\bar{h}/\sigma$, Γ being rate of flow, D_h hydraulic diameter and σ surface tension.

Equation [13] was statistically determined (correlation factor $r = 0.8$). In this way it represents an empirical relation. At this stage it was assumed that the incipient two and three dimensional wave was continuously developed with the increasing of the flow rates. Thus their geometry and dynamics aspects are identical with those of the wavelets in the disturbance wave region.

Experimental observations (Woodmansee & Hanratty 1969; Zanelli & Hanratty 1971) have confirmed that the atomisation is due to the breakdown of the wavelets superposed on the disturbance waves. It was an objective of this study to demonstrate that the droplet distribution can be correlated with the aid of above defined wave characteristics.

The velocity ($\bar{c}$) and the length ($\bar{\lambda}$) of the propagation wave could also be statistically correlated as a function of X as follows:

$$\frac{\bar{c}}{\bar{w}_G} = f_1(X); \quad \frac{\bar{\lambda}}{y_{\text{eff}}} = f_2(X). \qquad [14a,b]$$

The statistical analysis of the experimental data (Zanelli & Hanratty 1971) (referred to two and three dimensional wave and wavelet geometry) leads to the following empirical equations:

$$f_1(X) = 0.04X^{-1.246}; \quad f_2(X) = 21.035X^{-1.1959}. \qquad [15a,b]$$

4. EXPERIMENTAL

The direct investigation was performed in order to determine the correlation between wavy aspect versus the shear stress and void fraction distribution as well as the heat transfer rate.

Figure 2 illustrates schematically the experimental rig employed in the investigation.

The measurements were carried out in a horizontal channel of rectangular cross section of 100×80 mm (7 in figure 2). This ratio was chosen as presenting the possibility of analysing the droplet evolution and a better correlation of the data regarding the heat transfer. The three-dimensional character of the gas flow implied the necessity of performing the measurements in the longitudinal axial section. The main equipment consisting of a burning chamber (15) (used also for the droplet spray chamber), a calming section (14), the channel (7) and a droplet eliminator (5) that is joined by a suction line to fans (1).

The liquid (at this stage tap water and degassed water were used) was fed by means of a constant level tank (12) provided with a stirrer and thermostat, the liquid being withdrawn in a tank (17) connected to a vacuum pump.

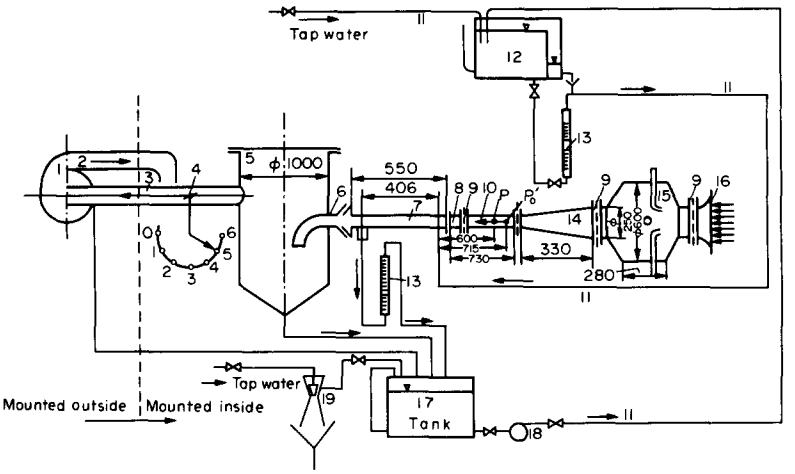

Figure 2. Schematic diagram of experimental rig.

The gas speed was in the range of 0.5–30 m/s and the water flow from 5 to 30 l/h.

The local void fraction distribution

A hot film wedge shaped probe (DISA-55A83) connected to a constant temperature anemometer (DISA-55D00) was used as a measuring device for droplet size.

The method principally consists of the analysis of the electric output signal whose amplitude (e_d) represents the droplet volume impacting and evaporating on the hot film of a probe. The amplitude of the output electric signal obtained by means of a constant temperature anemometer bridge (DISA-55D00) was analysed, and the signals within a certain range of values were counted.

The calibration was performed by means of an aerosol generator constructed in accordance with the British Standard 2831/1971, followed the method described by Goldschmidt & Householder (1968). The sensitivity of the system, S_d, was calculated under the following operating conditions: hot film temperature $t_h = 215°C$, respective hot probe resistance $R_H = 20.93\Omega$,

$$S_d = \left[\frac{(\rho C_p)_L \pi (T_a - T_b)}{2} \frac{tg\theta}{R_H k^2}\right]^{1/3} = \frac{e_d}{d_d}, \qquad [16]$$

where the droplet diameter is d_d and, the liquid density ρ_L and specific heat C_p, respectively were considered at the temperature $(T_a + T_b)/2$, T_a being the liquid droplet initial temperature and T_b the boiling temperature.

For pure water droplets at normal pressure, $S_d = 0.0195\ V/\mu m$. The slope angle θ of the anemometer experimental response curve, used in [16] was analysed from the galvanometer and direct print recording of the bridge output signal.

The sensitivity statistically obtained from calibration (up to 0.1 mm droplet diameter) was $0.018\ V/\mu m$. The slight deviation from calculated value was due, perhaps, to the droplets' deformation on the microscope trapping lamella.

The capture area from the hot film sensor was calculated by means of the following relation:

$$A_{ef\,cap} = (1 + d_p)\left(0.35 + \frac{3}{2}d_p\right) \quad (mm^2), \qquad [17]$$

where the net dimension of the hot film is $1 \times 0.35\ mm^2$ and d_p represents the diameter of the respective droplet. The capture area was considered the net probe area plus an area limited by $\frac{1}{2}d_p$ in the lower and side part of the probe, and d_p above the probe. The analysis was limited to the

four size ranges: $d_p > 0.767$; 0.510; 0.383; 0.255 and $d_p < 0.128$ mm, corresponding to the oscilloscope gates at 15; 10; 7.5; 5 and 2.5 V.

The droplets captured by the hot film which produced an output signal greater than the level of the oscilloscope fixed gate were automatically counted.

For each probe height position y above the plate, the liquid fraction $(1-\alpha)$ is:

$$(1-\alpha)_y = \frac{\frac{\pi}{6}\sum_0^i N d_i^3}{\bar{w}_y \tau A_{ef\,cap}}, \qquad [18]$$

where N is the number of droplets counted for each diameter range d_i (an average value was considered for each range), $\bar{w}_y$ is the axial velocity of air for the height position y, and τ is the total observation time.

Several void fraction distributions could be established for the various rates of gas liquid flows (each representing an independent run),

$$1-\alpha = Ky^{-k_2}. \qquad [19]$$

The exponential correlations as proven to be very satisfactory. By matching the measured outer film droplet distribution and that calculated in the wave affected region (by means of [13] and [15a,b]) there results the following overall liquid fraction distribution:

$$(1-\alpha) = \frac{WeX}{305} y'^{-0.092/y_{min}} \quad (r > 0.95) \qquad [20]$$

where $y' \geqslant e^{-(y_{min}/0.092)\ln(WeX/305)}$.

In this way, by a slight increase of the continuous liquid film level y_{min} (the increased value is under 1/1000 from the mean thickness of the film in all performed experiments), the liquid fraction value $(1-\alpha)$ in the [20] never exceeds 1.

Shear stress distribution

To integrate the shear stress equation a supplementary assumption is necessary concerning the distribution of ratio τ_y/τ_0 vs. y^+.

By assuming a linear distribution in the continuous liquid layer and a constant one in the dispersed core and wavy region it follows that:

$$\frac{\tau_y}{\tau_0} = 1 - \frac{y^+}{y^+_{min}}\left(1 - \frac{\tau_{02}}{\tau_{01}}\right), \quad (0 \leqslant y^+ \leqslant y^+_{min}) \qquad [21]$$

and we could also assume that $(y^+ \geqslant y^+_{min})$, where τ_{01} is the shear stress at the solid wall wetted by the flowing film and τ_{02} is the apparent shear stress reduced at the level $y^+ = y^+_{min}$.

The value of τ_{01} was measured by using a flush mounted hot film probe (DISA-55A91) connected to an anemometer bridge and the value τ_{02} was separately computed. Some previous results (Webb, Eckert & Goldstein 1971) concerning the friction characteristics in the repeated rib roughness surface were also used for this purpose.

The calibration operation of the flush mounted hot film probe was performed in a water (degassed) fed microtunnel. The calibration in the water microtunnel and the one in the film condition are restricted by the laminar flowing condition in vicinity of hot film (Belhouse & Schultz 1966).

$$w^* l/\nu_L > 6.6 Pr_L^{1/2}; \quad w^* l/\nu_L < 64 Pr_L. \qquad [22]$$

Another restriction is on the film thickness (Toma 1974), which should be greater than thermal ɔundary layer thickness.

Based on the above mentioned conditions we obtain the following limits:

°C	Lower limit (N/m^2)	Upper limit (N/m^2)
20	0.010	203.78
80	$2.53 \cdot 10^{-3}$	2.60

The calibration function thus obtained is:

$$\rho_0 = (321.8K_i - 0.721)^3 \quad N/m^2, \tag{23}$$

here

$$K_1 = \frac{V_B^2}{332.11} \frac{1}{T_B - T_0}.$$

The statistical analysis (based on 102 runs) of the anemometer output voltages V_B leads to a ıtisfactory linear approximation:

$$\tau_{01} = 4.560X - 0.933 \quad N/m^2, \tag{14}$$

$$(r = 0.86),$$

$$(\text{for the } 0.1 < X < 0.8).$$

A less strong correlation was obtained for all other tested linear functions of the type:

$$y_1 = ax_1 + b, \tag{25a,b}$$

vhere

$$y_1 = \frac{\tau_{01}}{hX}; \quad x_1 = \frac{\rho \bar{w}_L^2}{Re_L^n X \bar{h}}.$$

For example, the better one was:

$$\tau_{01} = 8.036\left(\frac{\rho}{8} w_L^2 \frac{0.355}{Re_L^{0.261}}\right) + 1.088 \quad N/m^2, \tag{26}$$

$r = 0.786$).

Other types of correlations, such the exponential, were also computed, which led to much lower ɔorrelation factors.

The shear stress at the fluid interface (τ_{02}) was computed for the range $10 < (\bar{\lambda}/e) < 40$, $\cdot^+ > 35$, using the relations (Webb, Eckert & Goldstein 1971):

$$(2/f)^{1/2} = 2.5 \ln (D_h/2e) - 3.75 + 0.95(\bar{\lambda}/e)^{0.53}, \tag{27}$$

ınd the investigated repeated rib dimensions were replaced by the length and amplitude limensions of the model:

$$\frac{\bar{\lambda}}{e} = \frac{\bar{\lambda}}{y_{\text{eff}}\sqrt{(2)}}, \tag{28}$$

where $\bar{\lambda}$ is the repeated rib period and e the height of a small obstacle of well defined periodicity. The friction factor f is correlated by the shear stress τ_{02} by means of [29]:

$$\tau_{02} = \frac{\rho_{2E}\bar{W}_G^2}{8} f. \qquad [29]$$

Thus it is assumed at this stage, that the repeated rib experienced in one phase pressure loss determination has an effect (i.e. a super-position of equivalent sand roughness and recirculation pattern) similar to that of the modeled waves.

An air–water droplet system was considered with local properties given by [6] at a temperature

$$t_{2F} = \frac{t_S + \frac{t_G + t_L}{2}}{2},$$

where S denotes the saturation condition. A computation program was developed and applied to the 102 runs previously used for the wall shear stress measurements.

Figure 3 presents the ratio τ_{02}/τ_{01}, as a function of the factor X.

The strong correlation is demonstrated by the two linear dependencies:

$$\frac{\tau_{02}}{\tau_{01}} = 6.718X - 0.591 \quad (X > 0.285)$$

$$r = 0.948,$$

$$\frac{\tau_{02}}{\tau_{01}} = 40.425X + 12.854 \quad (X \leqslant 0.285)$$

$$r = 0.824. \qquad [30a,b]$$

The heat transfer from hot bottom channel plate to the horizontal flowing liquid film

The Plexiglas tunnel zone (7 in figure 2) in which the droplet distribution and shear stress measurements were performed was replaced with a stainless steel zone of the same size (figure 4).

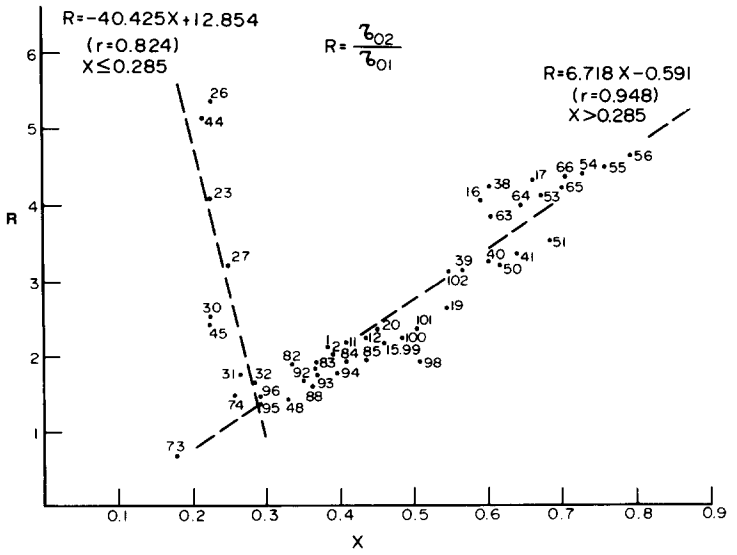

Figure 3. The film shear stress ratio vs. wavy factor X.

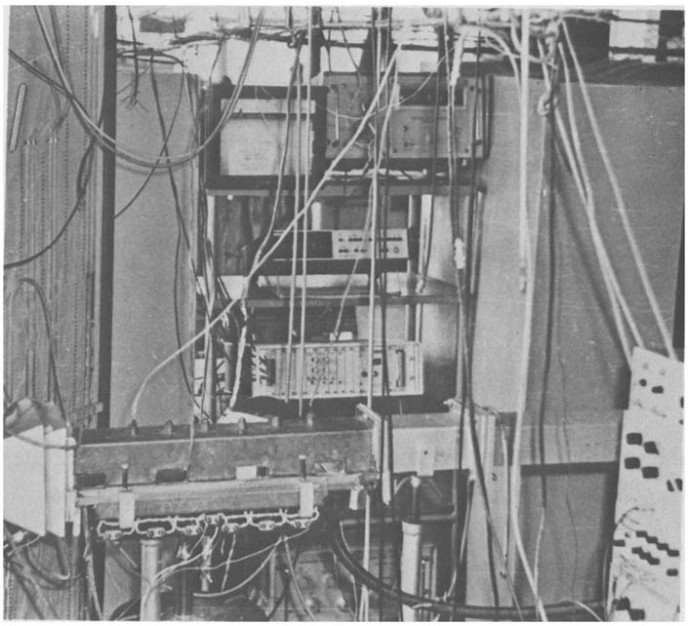

Figure 4. A view of the tunnel arrangement in a heat-transfer measurement.

The heat flux was supplied by a controlled electric heater with a device for external loss compensation. Both the inlet–outlet liquid film bulk temperatures and four point wall temperatures were recorded (using Philips stick-on thermocouples, NiCr–Ni 0.2 mm thick, and sheathed Cromel–Alumel 0.3 mm dia.). A data logging unit allowed the recording of all thermocouple e.m.f.'s with a precision of $\pm 0.5\ \mu$V.

Calibration was against standard with an accuracy of ±0.05°C. All the runs were analysed on an IBM-360 computer by means of statistical multiple regression (free optimal and forced). The function analysed was of the type:

$$Nu = f\left(Re_L : Pr_L ; We ; X ; \frac{U_L}{U_{0L}} ; \frac{\tau_{02}}{\tau_{01}} \ldots\right).$$

Table 1 presents the sequence of selection for the optimal correlation and the respective correlation factor.

Table 1.

$Nu =$	$f\left[Re_L$ and $\frac{\mu_L}{\mu_{0L}}$ and $\frac{\tau_{02}}{\tau_{01}}$ and X and $We \ldots\right]$				
The sequence in optimal regression	1	2	3	4	5
The complex correlation factor (r')	0.908	0.954	0.9949	0.995	0.9955

For the experimental data provided in the range $X > 0.285$ the following relation is computed:

$$Nu = 8.945 \cdot 10^{-2} Re_L^{0.717} (\mu_L/\mu_{0L})^{-10.76} (\tau_{02}/\tau_{01})^{-0.883}. \quad (r' = 0.995). \qquad [31]$$

As (τ_{02}/τ_{01}) is a unique function of X, the dependence between the wavy aspect and the heat transfer is implicitly evinced. An explicit relation was computed by means of a forced induced

variable in a statistical correlation:

$$Nu = 6.339 \times 10^{-4} Pr_L^{0.967} Re_L^{0.835} X^{-0.54} \quad (r' = 0.915), \qquad [32]$$

$$X \geqslant 0.285.$$

All the parameters in [31] and [32] were computed for the bulk liquid film temperature. The lack of data in the investigated flow range did not enable a numerical comparison of the results.

5. CONCLUDING REMARKS

1. A new function X statistically characterizing the wavy aspect of the two and three dimensional wavy flow is presented.

2. The function X closely correlates the phenomena taking place in the squalled wavy flow as well as those in the disturbance wave regime. This points out the fact that the wavelet induced mechanisms are similar to those of the two and three dimensional incipient waves.

3. The analytical description of the system is performed in terms of the one phase "law of the wall" equations provided that the wavy sinusoidal model and the limit of integration (continuous liquid sublayer and wavy-dispersed core) are also included.

4. The void fraction in the core and in the wavy region is representable by a unique exponential function depending on the We number, the continuous sublayer thickness y'_{min}, and the wavy function X.

5. The shear stress ratio (τ_{02}/τ_{01}) is a unique function of X denoting a minimum value (at the investigated air–water film system $(\tau_{02}/\tau_{01})|_{min}^{X_L=0.285}$).

6. The heat-transfer coefficient from the wall to the film is experimentally determined as a function of shear stress ratio (τ_{02}/τ_{01}) and/or X.

7. The mean film thickness previously determined as a function of dry wall shear stress (van Rossum' 1959 experimental correlation) becomes an implicit function of X, thus expressing the phase interaction.

8. The results of this study contribute to a more realistic basis for the future investigation and engineering computation in the two-phase liquid film dispersed systems.

REFERENCES

BELHOUSE, B. J. & SCHULTS, D. L. 1966 Determination of mean and dynamic skin friction—separation and transition in low-speed flow with thin-film heated element. *J. Fluid Mech.* **24**, 379–400.

BIASI, L., CLERICI, G. C., SALA, R. & TOZZI, A. 1968 Studies on film thickness and velocity distribution of two-phase annular flow. Rep. EUR-3765e, Instituto di Science Fisiche Univ. Milano ARS-SpA.

CHANG, F. W. & DUKLER, A. E. 1964 The influence of a wavy, moving interface on pressure drop for flow in conduits. *Int. J. Heat Mass Transfer* **7**, 1395–1404.

CLEGG, M. J. & TAIT, R. W. 1962 The application of Dukler analysis to the falling film evaporate. Personal Communication. *Chem. Eng. Dept. Univ. of Adelaide.*

DEISSLER, R. G. 1955 Analysis of turbulent heat transfer, mass transfer and friction in smooth tubes at high Prandtl and Schmidt number. NACA Rep. 1210.

DELHAYE, J. M. 1968 Measure du taux de vide local en écoulement diphasique eau–air par un anémomètre à film chaud. Rapport CEA-R-3465. Centre d'Etudes Nucléaires de Grenoble.

DUKLER, A. E. 1960 Fluid mechanics and heat transfer in vertical falling-film systems. CEP Symp. Series 56, No. 30, 1–10.

DUKLER, A. E., MOYE WICKS, III & CLEVELAND, R. G. 1964 Frictional pressure drop in two-phase flow. *A.I.Ch.E. JL.* A. **10**, 38–44, B. **10**, 44–51.

FRISK, D. P. & DAVIS, E. J. 1972 The enhancement of heat transfer by waves in straitified gas-liquid flow. *Int. J. Heat Mass Transfer* **15**, 1537–1552.

GATER, R. A. & L'ECUYER, M. R. 1970 A fundamental investigation of the phenomena that characterize liquid film cooling. *Int. J. Heat Mass Transfer* **13**, 1925–1939.

GOLDSCHMIDT, V. E. & HOUSEHOLDER, M. K. 1968 Measurements of aerosols by hot wire anemometry. In *Advances in Hot-Wire Anemometry*. AFOSR 68–1492, 135–152.

HANRATTY, T. J. & ENGEN, J. M. 1957 Interaction between a turbulent air stream and a moving water surface. *A.I.Ch.E.Jl.* **3**, 299–304.

LEVY, S, 1966 Prediction of two-phase annular flow with liquid entrainment. *Int. J. Heat. Mass Transfer* **9**, 171–188.

LILLELEHT, V. L. & HANRATTY, T. J. 1963 Measurement of interfacial structure for co-current air–water flow. *J. Fluid Mech.* **11**, 65–81.

LOCKHART, R. W. & MARTINELLI, R. C. 1949 Proposed correlation of data for isothermal two-phase two-component flow in pipes. *Chem. Engng Prog.* **45**, 39–48.

OSTRACH, S. & KOESTEL, A. 1965 Film instabilities in two-phase flows. *A.I.Ch.E.Jl.* **11**, 294–303.

PIMSNER, V. & TOMA, P. 1970 Metode de măsurare a grosimii filmelor lichide. *Studii Cerc. energ. electrotehnice* **20**, 43–52.

PIMSNER, V. & TOMA, P. 1974 The wavy aspect of a two-phase liquid film flow system. *Rev. Roum. Sci. Tech. Electrotech. Energ.* **19**, 153–162.

VAN ROSSUM, J. 1959 Experimental investigation of horizontal liquid films—wave formation, atomization, film thickness. *Chem Engng Sci.* **11**, 35–52.

TELLES, A. S. & DUKLER, A. E. 1970 Statistical characteristics of thin, vertical, wavy, liquid films. *IEC Fundamentals* **9**, 412–421.

TOMA, P. 1974 On the heat and mass transfer between a gas and a liquid film co-currently flowing on a horizontal flat plate. Doctoral diss. Politechnical Institute Bucharest.

WEBB, R. L., ECKERT, E. R. G. & GOLDSTEIN, J. J. 1971 Heat transfer and friction in tubes with repeated-rib roughness. *Int. J. Heat Mass Transfer* **14**, 601–617.

WOODMANSEE, D. E. & HANRATTY, T. J. 1969 Mechanism for the removal of droplets form a liquid surface by a parallel air flow. *Chem. Engng Sci.* **24**, 299–307.

ZANELLI, S. & HANRATTY, T. J. 1971 Relationship of entrainment to wave structure on a liquid film. Int. Symposium on Two-Phase Systems, Technion City, Haifa, Israel.